

# Theory of nuclear relaxation in superconducting high-T<sub>c</sub> oxides

著者	Koyama T., Tachiki M.
journal or publication title	Physical Review. B
volume	39
number	4
page range	2279-2292
year	1989
URL	<a href="http://hdl.handle.net/10097/53319">http://hdl.handle.net/10097/53319</a>

doi: 10.1103/PhysRevB.39.2279

## Theory of nuclear relaxation in superconducting high- $T_c$ oxides

T. Koyama and M. Tachiki

*Institute for Materials Research, Tohoku University, 2-1-1 Katahira, Sendai 980, Japan*

(Received 15 June 1988; revised manuscript received 19 September 1988)

In connection with the anomalous temperature dependence of the nuclear relaxation rate  $1/T_1$  of Cu in  $\text{YBa}_2\text{Cu}_3\text{O}_{7-y}$ , the nuclear relaxation in the system is theoretically investigated, and the anomalous temperature dependence is found to be explained on the basis of the Bardeen-Cooper-Schrieffer (BCS) pairing, if the strong correlation effect of electrons is properly taken into account. The spin fluctuations make the superconducting state gapless near  $T_c$  and erase the hump of  $1/T_1$  which is usually observed in BCS superconductors. The spin-fluctuation vertex is highly renormalized in the superconducting state and thus  $1/T_1$ , enhanced by the spin fluctuations in the normal state, is drastically suppressed in the superconducting state. The above two effects combined give a sharp decrease of  $1/T_1$  below  $T_c$ , which has been observed in the superconducting state of  $\text{YBa}_2\text{Cu}_3\text{O}_{7-y}$ .

### I. INTRODUCTION

Extensive experimental and theoretical studies to elucidate the mechanism of the high- $T_c$  superconductivity of the superconducting oxides have been made.<sup>1</sup> The experimental results show that the electrons in the oxides are highly correlated due to the Coulomb correlation. Actually,  $\text{La}_2\text{CuO}_4$  and  $\text{YBa}_2\text{Cu}_3\text{O}_6$  are insulators due to the correlation, although band calculations show that these crystals are metallic. The insulating crystals exhibit antiferromagnetic orders of copper spins. If holes are doped into the crystals, the antiferromagnetic orders rapidly destruct and, simultaneously, the electrical conductivity increases. In this case we expect the appearance of a Fermi-liquid state near the Fermi level. The characteristic feature of the Fermi liquid is the following. The copper  $d$ -electron levels are close to the oxygen  $p$ -electron levels in these oxides, unlike in other transition-metal oxides. Therefore, electrons can move around the crystals on the hybridized orbits constituted from the copper  $d$ -electron and oxygen  $p$ -electron orbits. The electrons in the Fermi liquid are heavily dressed by charge and spin fluctuations, since the large fluctuations are expected in such correlated systems.

The measurement of the flux quantization<sup>2</sup> and the ac Josephson effect<sup>3,4</sup> show that the unit of the superconducting current in the oxides is twice the electronic charge. This fact indicates that electron pairs or hole pairs are responsible for superconductivity even in the oxide superconductors. The coherence lengths estimated from the upper critical fields are 30 to 40 Å in the basal planes of  $\text{YBa}_2\text{Cu}_3\text{O}_{7-y}$  (Refs. 5 and 6) and  $\text{Bi-Sr-Ca-Cu-O}$ .<sup>7</sup> These values are shorter than those in usual superconductors, but much longer than the distance between Cu and O ions in the crystals which is approximately 2 Å. Therefore, there is nothing wrong in considering the Bardeen-Cooper-Schrieffer (BCS)-type pairing in the oxides. The specific heat of  $\text{YBa}_2\text{Cu}_3\text{O}_{7-y}$  shows a sharp jump at the superconducting transition temperature  $T_c$ .<sup>8</sup> This specific heat can be explained on the basis of the BCS theory, if the large contribution from the superconducting fluctuations as a result of the short coherence length is included.<sup>9</sup>

The experimental results of the tunneling using  $\text{La}_{2-x}\text{Sr}_x\text{CuO}_4$  and  $\text{YBa}_2\text{Cu}_3\text{O}_{7-y}$  show the clear energy gaps which are expected from the BCS theory.<sup>10</sup> The temperature dependence of the penetration depth in  $\text{YBa}_2\text{Cu}_3\text{O}_{7-y}$  measured by muon-spin rotation is consistent with the prediction by the BCS theory.<sup>11-13</sup>

Only the experimental results which look inconsistent with the BCS-type pairing are the result of nuclear relaxation. Warren *et al.*,<sup>14</sup> Mali *et al.*,<sup>15</sup> Kitaoka, Hiramatsu, Kondo, and Asayama,<sup>16</sup> and Imai *et al.*<sup>17</sup> made the nuclear quadrupole resonance (NQR) measurements of  $\text{YBa}_2\text{Cu}_3\text{O}_{7-y}$ . They obtained almost the same results on the nuclear relaxation of Cu in the two-dimensional  $\text{CuO}_2$  layers of the crystals which is called Cu II. The superconducting current is considered to flow mainly in these layers. For these reasons we focus on the nuclear relaxation of Cu II hereafter. The behavior of the nuclear relaxation rate  $1/T_1$  differs from that in usual BCS superconductors in the following points. (1) The hump of  $1/T_1$  which is usually seen just below  $T_c$  in the BCS superconductors is not observed.<sup>14-17</sup> (2) The relaxation rate  $1/T_1$  sharply decreases below  $T_c$ .<sup>14-17</sup> Its temperature dependence is expressed by a power of temperature  $T^n$  rather than an exponential, and the value of  $n$  is 4.5 and 3 depending on the temperature range.<sup>17</sup> (3) The relaxation rate  $1/T_1$  in the normal state is approximately proportional to  $T^{1/2}$  between 92 and 200 K.<sup>17</sup>

To explain the anomalous temperature dependence of the nuclear relaxation rate mentioned above, Kitaoka *et al.*<sup>16</sup> used an anisotropic energy-gap function with  $d$ -wave symmetry, and Suzumura, Hasegawa, and Fukuyama<sup>18</sup> considered the resonating-valence bond (RVB) superconducting state with  $d$ -wave symmetry. They all use the mean-field approximation for the calculation of the nuclear relaxation rate. However, we cannot use the simple mean-field approximation in the calculation of quantities in highly correlated systems such as the oxide superconductors. The objective of the present paper is to show that the anomalous temperature dependence of the nuclear relaxation mentioned above can be explained on the basis of the BCS theory, if the correlation effect is properly taken into account.

The following is a brief explanation for our mechanism of the nuclear relaxation. It has been confirmed from the experiments that the relaxation of the CuII nuclei is caused by a magnetic origin in entire temperature range.<sup>17</sup> In this case,  $1/T_1$  is expressed in terms of the imaginary part of the dynamical spin susceptibility of electrons with the resonance frequency. The imaginary part of the susceptibility in the copper oxide system is calculated using the following model. Due to the strong repulsive interaction between the electrons on copper ion sites, the states situated deeply below the Fermi level are almost localized at the lattice sites, consistent with the experimental results of photoemission. In the metallic sample, along with this localized state, the Fermi-liquid state appears near the Fermi level. Some attractive interaction between the quasielectrons yields the superconducting state in the Fermi liquid. In the system, the spins of copper ions are almost localized at the lattice sites and only a small portion of the spin are itinerant. These spins produce the large spin fluctuations. The spin fluctuations create a self-energy of the quasielectron. Especially, its imaginary part works to shorten the lifetime of the quasielectron. This lifetime effect makes the superconducting state gapless near  $T_c$  and erases the hump in the  $1/T_1$  vs  $T$  curve. The susceptibilities at low frequencies are enhanced by scattering of the spin fluctuations and the quasielectrons in the normal state. However, when the superconducting order parameter develops, the low-frequency part of the spin-fluctuation vertex for the scattering is very much reduced and thus the enhancement of the susceptibility is drastically suppressed. The above two effects combined cause the drastic decrease of  $1/T_1$  without accompanying a hump, just as observed in the NQR experiments of CuII in  $\text{YBa}_2\text{Cu}_3\text{O}_{7-y}$ . Since the gapless state appears only near  $T_c$ , the present result is consistent with the observations of the energy gap by the tunneling and optical measurements at low temperatures.<sup>10</sup>

## II. EFFECTS OF SPIN FLUCTUATIONS ON THE ONE-ELECTRON STATES IN THE SUPERCONDUCTING STATE

Assuming that the superconductivity in the oxides is brought about by a certain interaction other than one via spin fluctuations, we consider the following model described by the Hamiltonian

$$H = H_{\text{super}} + \int d^3x U \psi^\dagger(x) \psi^\dagger(x) \psi_1(x) \psi_1(x), \quad (2.1)$$

where  $U$  and  $\psi_\sigma(x)$  are, respectively, the correlation interaction energy constant and the field operator for the conduction electrons with spin  $\sigma$ . In (2.1)  $H_{\text{super}}$  denotes the part which is responsible for the superconductivity and the second term represents the on-site Coulomb repulsive interaction, i.e.,  $U > 0$ . For the calculations of physical quantities at finite temperatures we utilize the formula-

tion of thermofield dynamics (TFD).<sup>19,20</sup> Following the TFD formalism, we introduce the Heisenberg field  $\tilde{\psi}_\sigma(x)$  which anticommutes with  $\psi_\sigma(x)$  to incorporate the temperature effect. Then our system is described by the total Hamiltonian

$$\hat{H} = H - \tilde{H}, \quad (2.2)$$

where

$$\tilde{H} = \tilde{H}_{\text{super}} + \int d^3x U \tilde{\psi}^\dagger(x) \tilde{\psi}^\dagger(x) \tilde{\psi}_1(x) \tilde{\psi}_1(x). \quad (2.3)$$

We define the thermal doublet:

$$\Psi_\sigma^\alpha(x) = \begin{cases} \psi_\sigma(x) & \text{for } \alpha=1, \\ \tilde{\psi}_\sigma^\dagger(x) & \text{for } \alpha=2, \end{cases} \quad (2.4)$$

and, in the Nambu representation,

$$\Psi^\alpha(x) = \begin{pmatrix} \psi_1^\alpha(x) \\ \psi_2^\alpha(x) \end{pmatrix} = \begin{pmatrix} \psi_1^\alpha(x) \\ \psi_1^\alpha(x)^\dagger \end{pmatrix}. \quad (2.5)$$

Hamiltonian (2.2) leads to the equation for  $\Psi^\alpha(x)$  as

$$[i\partial_t - \varepsilon(-\nabla^2) \tau_3] \Psi^\alpha(x) = J(\Psi^\alpha, \Psi^{\alpha\dagger}) - iU \sigma_\alpha^\alpha(x) \tau_2 \Psi^\alpha(x)^\dagger, \quad (2.6)$$

where  $\varepsilon(-\nabla^2)$  is the bare one-electron energy,  $\tau_i$ 's ( $i=1,2,3$ ) are the Pauli matrices,  $J[\Psi^\alpha, \Psi^{\alpha\dagger}]$  represents the interaction arising from the interaction term in  $H_{\text{super}} - \tilde{H}_{\text{super}}$ , and  $\Psi^\alpha(x)$  denotes the doublet transposed in the Nambu space,

$${}^t\Psi^\alpha(x) = [\psi_1^\alpha(x), \psi_2^\alpha(x)], \quad (2.7)$$

$${}^t\Psi^\alpha(x)^\dagger = \begin{pmatrix} \psi_1^\alpha(x)^\dagger \\ \psi_2^\alpha(x)^\dagger \end{pmatrix}, \quad (2.8)$$

and  $\sigma_\alpha^\alpha$  is given by

$$\sigma_\alpha^\alpha(x) = \varepsilon^\alpha \psi_1^\alpha(x)^\dagger \psi_2^\alpha(x) = -\frac{i}{2} \varepsilon^\alpha {}^t\Psi^\alpha(x) \tau_2 \Psi^\alpha(x), \quad (2.9)$$

with

$$\varepsilon^\alpha = \begin{cases} 1 & \text{for } \alpha=1, \\ -1 & \text{for } \alpha=2. \end{cases} \quad (2.10)$$

To investigate the one-electron state in our system, we first calculate the one-electron Green's function. In the TFD formalism the causal Green's function at temperature  $T$  is defined by

$$S_{ab}^{\alpha\beta}(x-y) = \langle O(\beta) | T \Psi_a^\alpha(x) \Psi_b^\beta(y)^\dagger | O(\beta) \rangle = \frac{i}{(2\pi)^4} \int d^4p S_{ab}^{\alpha\beta}(p) e^{ip(x-y)}, \quad (2.11)$$

$|O(\beta)\rangle$  being the temperature-dependent vacuum state ( $\beta=1/T$ ). Using Eq. (2.6), we obtain the equation for  $S^{\alpha\beta}(x-y)$ ,

$$[i\partial_t - \varepsilon(-\nabla^2) \tau_3] S^{\alpha\beta}(x-y) = i\delta^{\alpha\beta} \delta^{(4)}(x-y) + \langle O(\beta) | T J[\Psi^\alpha(x), \Psi^\alpha(x)^\dagger] \Psi^\beta(y)^\dagger | O(\beta) \rangle - iU \langle O(\beta) | T \sigma_\alpha^\alpha(x) [\tau_2 {}^t\Psi^\alpha(x)^\dagger] \Psi^\beta(x)^\dagger | O(\beta) \rangle. \quad (2.12)$$

If the self-energy functions  $\Xi^{a\beta}(p)$  and  $\Pi^{a\beta}(p)$  are respectively introduced by the relations

$$\langle O(\beta) | T J [\Psi^a(x), \Psi^a(x)^\dagger] \Psi^\beta(y)^\dagger | O(\beta) \rangle = \frac{i}{(2\pi)^4} \int d^4p \sum_\gamma \Xi^{\alpha\gamma}(p) S^{\gamma\beta}(p) e^{ip(x-y)}, \quad (2.13)$$

and

$$-iU \langle O(\beta) | T \sigma_z^a(x) [\tau_2 \Psi^a(x)^\dagger] \Psi^\beta(x)^\dagger | O(\beta) \rangle = \frac{i}{(2\pi)^4} \int d^4p \sum_\gamma \Pi^{\alpha\gamma}(p) S^{\gamma\beta}(p) e^{ip(x-y)}, \quad (2.14)$$

Eq. (2.12) becomes

$$\sum_\gamma [(p_0 - \varepsilon_p \tau_3) \delta^{\alpha\gamma} - \Xi^{\alpha\gamma}(p) - \Pi^{\alpha\gamma}(p)] S^{\gamma\beta}(p) = \delta^{\alpha\beta} \quad (2.15)$$

with

$$\varepsilon_p = p^2/2m - \mu.$$

Now let us consider the self-energy function (2.14). Since the correlation creates the large spin fluctuations in the low-energy region, we express  $\Pi^{a\beta}(p)$  in terms of the spin-fluctuation Green's function  $\chi^{a\beta}(q)$ . To do so, by introducing the spin-fluctuation vertex function  $\Gamma^{\xi;\eta\zeta}(-p; p-q)$ , we write three-point function  $\langle O(\beta) | T \sigma_z^a(z) \Psi^a(x)^\dagger \Psi^\beta(y) | O(\beta) \rangle$  in terms of  $\chi^{a\beta}(q)$  as follows:

$$\begin{aligned} \langle O(\beta) | T \sigma_z^a(z) \Psi^a(x)^\dagger \Psi^\beta(y) | O(\beta) \rangle = & \left[ \frac{i}{(2\pi)^4} \right]^2 \int d^4p d^4q [-\varepsilon^{\alpha\gamma} S^{\alpha\gamma}(p) \tau_2 S^{\alpha\beta}(p-q) \\ & + i \sum_{\xi,\eta} \chi^{\xi\alpha}(q) S^{\eta\gamma}(-p) \Gamma^{\xi;\eta\zeta}(-p; p-q) S^{\zeta\beta}(p-q)] e^{ipx - iqx - i(p-q)y}, \end{aligned} \quad (2.16)$$

where  $S^{a\beta}(p)$  and  $\Gamma^{\xi;\eta\zeta}(-p; p-q)$  are, respectively, the transposed Green's function and spin-fluctuation vertex function in the Nambu representation

$$S_{ab}^{a\beta}(p) \equiv S_{ba}^{\beta a}(p), \quad (2.17)$$

$$\Gamma_{ab}^{\xi;\eta\zeta}(-p; p-q) \equiv \Gamma_{ba}^{\xi;\eta\zeta}(-p; p-q), \quad (2.18)$$

and  $\chi^{a\beta}(q)$  is defined by

$$\chi^{a\beta}(x-y) \equiv \langle O(\beta) | T \sigma_z^a(x) \sigma_z^\beta(y) | O(\beta) \rangle = \frac{i}{(2\pi)^4} \int d^4q \chi^{a\beta}(q) e^{iq(x-y)}. \quad (2.19)$$

The first and second terms in the integrand on the right-hand side of Eq. (2.16) represent, respectively, the improper and proper parts of the three-point function [see Fig. 1(a)]. Noting the definition of  $\Pi^{a\beta}(p)$  given in Eq. (2.14), we obtain from Eq. (2.16)

$$\Pi^{a\beta}(p) = -U \left[ \frac{i}{(2\pi)^4} \right] \int d^4q \varepsilon^{\alpha\gamma} \tau_2 S^{\alpha\alpha}(-p-q) \tau_2 \delta^{\alpha\beta} + U \left[ \frac{i}{(2\pi)^4} \right] \int d^4q \sum_{\xi,\gamma} \tau_2 S^{\gamma\alpha}(-p-q) \Gamma^{\xi;\gamma\beta}(-p-q; p) \chi^{\xi\alpha}(q). \quad (2.20)$$

In Fig. 1(b) we show the graphical representation of Eq. (2.20). In the following calculations we employ the one-loop approximation for Eq. (2.20). As discussed in Refs. 21 and 22 the one-loop approximation gives a good description for strongly correlated systems such as the heavy-fermion systems in the low-energy region. The vertex function is then approximated in the following form by introducing the renormalized coupling constant  $U_r$ :

$$U \Gamma^{\xi;\gamma\beta}(-p-q; p) \approx U_r \tau_2 \delta^{\gamma\xi} \delta^{\xi\beta} \tau_2. \quad (2.21)$$



FIG. 1. Feynman diagrams for (a) the three-point function and (b) the self-energy function  $\Pi^{a\beta}(p)$ .

Thus, in the one-loop approximation we have

$$\Pi^{a\beta}(p) = \Pi_{\text{Hartree}}^{a\beta} - U_r^2 \left( \frac{i}{(2\pi)^4} \right) \int d^4q \tau_2 {}^t S^{\beta a}(-p-q) \tau_2 \chi^{\beta a}(q), \quad (2.22)$$

where

$$\Pi_{\text{Hartree}}^{a\beta} = -U \left( \frac{i}{(2\pi)^4} \right) \int d^4q \varepsilon^a \tau_2 {}^t S^{aa}(-q) {}^t \tau_2 \delta^{a\beta}. \quad (2.23)$$

The relation between  $U$  and  $U_r$  is given in Sec. III. Using the spectral representation for  $S^{a\beta}(p)$  and  $\chi^{a\beta}(q)$  (Refs. 20 and 23), we can obtain the following spectral representation of the self-energy function  $\Pi^{a\beta}(p)$ :

$$\Pi^{a\beta}(p) = \Pi_{\text{Hartree}}^{a\beta} + \int d\omega \Omega(\omega, \mathbf{p}) \left[ U_F(\omega) \begin{pmatrix} \frac{1}{p_0 - \omega + i\delta} & 0 \\ 0 & \frac{1}{p_0 - \omega - i\delta} \end{pmatrix} U_F^\dagger(\omega) \right]^{a\beta}, \quad (2.24)$$

where

$$\Omega(p_0, \mathbf{p}) = U_r^2 \int dq_0 \int \frac{d^3q}{(2\pi)^3} [\tau_2 {}^t \rho(-p-q) \tau_2 D(q)] [f_B(q_0) + f_F(p_0 + q_0)], \quad (2.25)$$

$$U_F(\omega) = \begin{pmatrix} c_F(\omega) & d_F(\omega) \\ -d_F(\omega) & c_F(\omega) \end{pmatrix}, \quad (2.26)$$

with

$$f_B(p_0) = \frac{1}{e^{p_0/T} - 1}, \quad f_F(p_0) = \frac{1}{e^{p_0/t} + 1}, \quad (2.27)$$

$$c_F^2(p_0) = 1 - f_F(p_0), \quad d_F^2(p_0) = f_F(p_0). \quad (2.28)$$

In Eq. (2.25)  $\rho(p)$  and  $D(q)$  are the spectral functions, respectively, for  $S^{a\beta}(p)$  and  $\chi^{a\beta}(q)$ . Note that  $\rho(p)$  is a  $2 \times 2$  matrix in the Nambu representation.

The spectral function (2.25) can be rewritten in the form

$$\Omega(p_0, \mathbf{p}) = \Omega_0(p_0, \mathbf{p}) \tau_0 + \Omega_1(p_0, \mathbf{p}) \tau_1 + \Omega_3(p_0, \mathbf{p}) \tau_3, \quad (2.29)$$

where

$$\Omega_0(p_0, \mathbf{p}) = \frac{1}{2} U_r^2 \frac{1}{(2\pi)^3} \int d^4q T_r [\tau_2 {}^t \rho(-p-q) \tau_2 D(q)] [f_B(q_0) + f_F(p_0 + q_0)], \quad (2.30)$$

$$\Omega_1(p_0, \mathbf{p}) = -\frac{i}{2} U_r^2 \frac{1}{(2\pi)^3} \int d^4q T_r [\tau_3 {}^t \rho(-p-q) \tau_2 D(q)] [f_B(q_0) + f_F(p_0 + q_0)], \quad (2.31)$$

$$\Omega_3(p_0, \mathbf{p}) = -\frac{i}{2} U_r^2 \frac{1}{(2\pi)^3} \int d^4q T_r [\tau_1 {}^t \rho(-p-q) \tau_2 D(q)] [f_B(q_0) + f_F(p_0 + q_0)] \quad (2.32)$$

and  $\tau_0$  is the unit matrix. The self-energy function (2.24) can be separated into its real and imaginary parts as follows:

$$\Pi^{a\beta}(p) = \Pi_{\text{Hartree}}^{a\beta} + \int d\omega \frac{\Omega(\omega, \mathbf{p})}{p_0 - \omega} \delta^{a\beta} - i\pi \Omega(p_0, \mathbf{p}) [U_F(p_0) \hat{\varepsilon} U_F(p_0)^\dagger]^{a\beta}, \quad (2.33)$$

with

$$\hat{\varepsilon} = \begin{vmatrix} 1 & 0 \\ 0 & -1 \end{vmatrix}. \quad (2.34)$$

The real part of  $\Pi^{a\beta}(p)$  leads to the wave-function renormalization and the mass renormalization, so that the superconducting transition temperature  $T_c$  is decreased from that for  $U=0$ . On the other hand, the imaginary part of  $\Pi^{a\beta}(p)$  gives a finite lifetime to the quasiparticle in the superconducting state due to the process of emission and absorption of the spin fluctuations. As seen in the following this effect brings about a gapless superconducting state near  $T_c$  and plays a crucial role in the superconducting state of the superconducting oxides. We assume that the interaction term which leads to the self-energy function  $\Xi^{a\beta}(p)$  does not break the time-reversal symmetry. In this case  $\Xi^{a\beta}(p)$  have no imaginary part in the low-energy region below the superconducting energy gap in the absence of  $U$ . Hence, we approximate  $\Xi^{a\beta}(p)$  to be real and write it in the form

$$\Xi^{a\beta}(p) + \text{Re}\Pi^{a\beta}(p) = (1 - Z_p^{-1}) p_0 \tau_0 + c_p \tau_3 + \Delta_p \tau_1, \quad (2.35)$$

where  $Z_p$ ,  $c_p$ , and  $\Delta_p$  are real. Then Eq. (2.15) is rewritten as

$$\sum_{\gamma} [(Z_0^{-1} p_0 - \tilde{\epsilon}\tau - \Delta\tau) \delta^{\alpha\gamma} - i \text{Im}\Pi^{\alpha\gamma}(p)] S^{\gamma\beta}(p) = \delta^{\alpha\beta}, \quad (2.36)$$

with  $\tilde{\epsilon}_p = \epsilon_p - c_p$ . Expressing the imaginary part of  $\Pi^{\alpha\gamma}(p)$  in the form

$$\text{Im}\Pi^{\alpha\beta}(p) \approx -\pi[\Omega_0(p_0, \mathbf{p})\tau_0 + \Omega_1(p_0, \mathbf{p})\tau_1][U_F(p_0)\hat{\epsilon}U_F(p_0)^\dagger]^{\alpha\beta}, \quad (2.37)$$

where we dropped the contribution from the  $\tau_3$  component for simplicity as is usually done,<sup>24</sup> we obtain the spectral function  $\rho(p_0, \mathbf{p})$  from Eq. (2.36),

$$\rho(p_0, \mathbf{p}) = \frac{A^{(0)}(p)\tau_0 + A^{(3)}(p)\tau_3 + A^{(1)}(p)\tau_1}{\pi[(Z_p^{-2}p_0^2 - \tilde{\epsilon}_p^2 - \Delta_p^2 - \Omega_p^{(0)2} + \Omega_p^{(1)2})^2 + 4(Z_p^{-1}p_0\Omega_p^{(0)} + \Delta_p\Omega_p^{(1)})^2]}, \quad (2.38)$$

where

$$A^{(0)}(p) = (Z_p^{-2}p_0^2 + \tilde{\epsilon}_p^2 + \Delta_p^2 + \Omega_p^{(0)2} - \Omega_p^{(1)2})\Omega_p^{(0)} + 2Z_p^{-1}p_0\Delta_p\Omega_p^{(1)}, \quad (2.39)$$

$$A^{(3)}(p) = 2\tilde{\epsilon}_p(Z_p^{-1}p_0\Omega_p^{(0)} + \Delta_p\Omega_p^{(1)}), \quad (2.40)$$

$$A^{(1)}(p) = 2Z_p^{-1}p_0\Delta_0\Omega_p^{(0)} + (Z_p^{-2}p_0^2 - \tilde{\epsilon}_p^2 + \Delta_p^2 - \Omega_p^{(0)2} + \Omega_p^{(1)2})\Omega_p^{(1)}, \quad (2.41)$$

with  $\Omega_p^{(0)} \equiv \pi\Omega_0(p_0, \mathbf{p})$  and  $\Omega_p^{(1)} \equiv \pi\Omega_1(p_0, \mathbf{p})$ . Since the density of states  $N_s(p_0)$  is given by

$$N_s(p_0) = \frac{1}{2} \int \frac{d^3p}{(2\pi)^3} T_r[\rho(p_0, \mathbf{p})], \quad (2.42)$$

we have

$$\begin{aligned} N_s(p_0) &= \int \frac{d^3p}{(2\pi)^3} \frac{(Z_p^{-2}p_0^2 + \tilde{\epsilon}_p^2 + \Delta_p^2 + \Omega_p^{(0)2} - \Omega_p^{(1)2})\Omega_p^{(0)} + 2Z_p^{-1}p_0\Delta_p\Omega_p^{(1)}}{\pi[(Z_p^{-2}p_0^2 - \tilde{\epsilon}_p^2 - \Delta_p^2 - \Omega_p^{(0)2} + \Omega_p^{(1)2})^2 + 4(Z_p^{-1}p_0\Omega_p^{(0)} + \Delta_p\Omega_p^{(1)})^2]} \\ &= N(0) \left[ Q_p^{(0)} \left( \frac{(\alpha_p^2 + \beta_p^2)^{1/2} - \alpha_p}{2(\alpha_p^2 + \beta_p^2)} \right)^{1/2} + p_0 \left( \frac{(\alpha_p^2 + \beta_p^2)^{1/2} + \alpha_p}{2(\alpha_p^2 + \beta_p^2)} \right)^{1/2} \right], \end{aligned} \quad (2.43)$$

where

$$\alpha_p = Z_p^{-2}p_0^2 - \Delta_p^2 - \Omega_p^{(0)2} + \Omega_p^{(1)2}, \quad (2.44)$$

$$\beta_p = 2(Z_p^{-1}p_0\Omega_p^{(0)} + \Delta_p\Omega_p^{(1)}), \quad (2.45)$$

and  $N(0)$  is the density of states at the Fermi level in the normal state. In deriving (2.43) we neglected the momentum dependence of  $\Omega_p^{(0)}$  and  $\Omega_p^{(1)}$ . Consider the spectral functions of the self-energy functions (2.30) and (2.31). For the spectral function  $\rho(p_0, \mathbf{p})$  in the integrands we use the BCS spectral function

$$\rho(p_0, \mathbf{p}) = \frac{E_p + \tilde{\epsilon}_p\tau_3 + \Delta_p\tau_1}{2E_p} \delta(p_0 - e_p) + \frac{E_p - \tilde{\epsilon}_p\tau_3 - \Delta_p\tau_1}{2E_p} \delta(p_0 + E_p), \quad (2.46)$$

with

$$E_p = \sqrt{\tilde{\epsilon}_p^2 + \Delta_p^2}. \quad (2.47)$$

Substitution of Eq. (2.46) into Eq. (2.30) and (2.31) gives

$$\Omega_0(p_0, \mathbf{p}) = M_0(p_0, \mathbf{p}) + M_0(-p_0, \mathbf{p}), \quad (2.48)$$

$$\Omega_1(p_0, \mathbf{p}) = -M_1(p_0, \mathbf{p}) + M_1(-p_0, \mathbf{p}), \quad (2.49)$$

where

$$M_0(p_0, \mathbf{p}) = \frac{1}{2} U_r^2 \int \frac{d^3q}{(2\pi)^3} D(E_{p+q} + p_0, \mathbf{p}) [f_B(E_{p+q} + p_0) + f_F(E_{p+q})], \quad (2.50)$$

$$M_1(p_0, \mathbf{p}) = \frac{1}{2} U_r^2 \int \frac{d^3q}{(2\pi)^3} \frac{\Delta_{p+q}}{E_{p+q}} D(E_{p+q} + p_0, \mathbf{p}) [f_B(E_{p+q} + p_0) + f_F(E_{p+q})]. \quad (2.51)$$

Since the spectral function of the spin-fluctuation Green's function is well approximated by a Lorentzian form in the

low-energy region, we use the following approximate expression for  $D(q_0, \mathbf{q})$  in Eqs. (2.50) and (2.51):

$$D(q_0, \mathbf{q}) = \frac{-K_2(\mathbf{q})q_0}{[1 - U_r K_1(\mathbf{q})]^2 + [U_r \pi K_2(\mathbf{q})]^2}, \quad (2.52)$$

$$K_2(\mathbf{q}) = \int \frac{d^3 p}{(2\pi)^3} \frac{2T}{E_p E_{p+q}} (E_p E_{p+q} + \tilde{\epsilon}_p \tilde{\epsilon}_{p+q} + \Delta_p^2) \delta(E_p - E_{p+q}) \frac{\partial f_F(E_p)}{\partial E_p}, \quad (2.53)$$

$$K_1(\mathbf{q}) = \int \frac{d^3 p}{(2\pi)^3} \frac{1}{2E_p E_{p+q}} \left[ \frac{E_p E_{p+q} - \tilde{\epsilon}_p \tilde{\epsilon}_{p+q} - \Delta_p^2}{E_p + E_{p+q}} [f_F(E_p) + f_F(E_{p+q}) - 1] + \frac{E_p E_{p+q} + \tilde{\epsilon}_p \tilde{\epsilon}_{p+q} + \Delta_p^2}{E_p - E_{p+q}} [f_F(E_p) - f_F(E_{p+q})] \right], \quad (2.54)$$

For the functions  $K_1(\mathbf{q})$  and  $K_2(\mathbf{q})$  we assumed the same functional form as that in the random-phase approximation (RPA). In Fig. 2 we show the numerical results for the density of states, when we neglect the energy dependence of  $\Delta_p$  and assume that its temperature dependence follows the BCS gap equation and  $Z_p = 1$ . As seen in Fig. 2(a), the density of states is completely gapless near  $T_c$ . However, it rapidly approaches a BCS-like density of

states as temperature decreases. When the correlation is weak, the density of states is almost BCS-like in the entire temperature range as seen in Fig. 2(b). The gapless superconducting state in the highly correlated system is analogous to the state in the superconducting system with a sufficient amount of magnetic impurity doping.

In the present model calculation we assumed the ferromagnetic spin fluctuations as a result of using the RPA for  $K_1(\mathbf{q})$  and  $K_2(\mathbf{q})$ . However, even in the case of antiferromagnetic spin fluctuations the density of states curve is qualitatively the same as that in the present case because the antiferromagnetic spin fluctuations also bring about a finite imaginary part to the self-energy of the quasiparticles in the superconducting state.

The strong correlation between conduction electrons reduces the superconducting transition temperature  $T_c$  in our formulation. However,  $T_c$  is not so much reduced in the high- $T_c$  superconducting oxides in the following reason. In the oxides the conduction electrons are formed by  $p$  electrons in O ions and  $d$  electrons in Cu ions. The strong correlation exists between the  $d$  electrons. If the superconductivity is mainly maintained by the attractive interaction between the  $p$  electrons (holes), the transition temperature may not be so much reduced by the strong repulsive interaction on the Cu sites. A more realistic calculation explicitly including the effect of  $p$  electrons is now in progress.

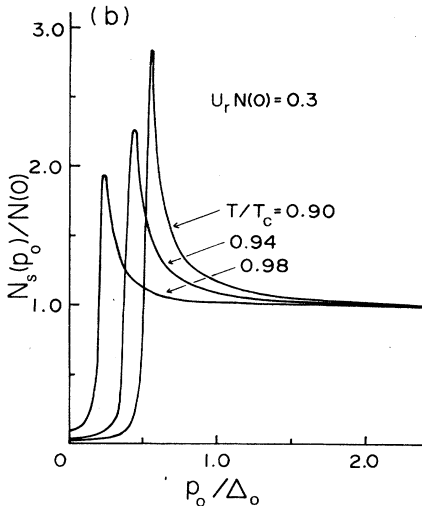
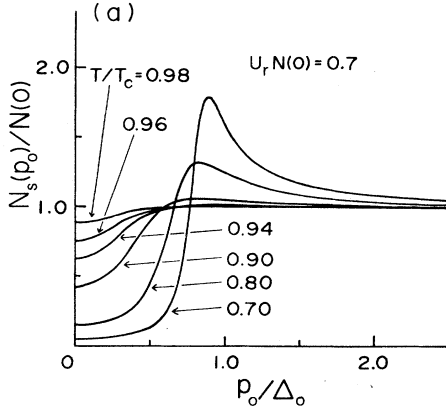


FIG. 2. Energy dependence of the density of states for various temperatures. (a)  $U_r N(0) = 0.7$ , (b)  $U_r N(0) = 0.3$ .

### III. CALCULATION OF THE LONGITUDINAL NUCLEAR RELAXATION TIME $T_1$

#### A. Formulation

In this section, based on the results given in Sec. II, we calculate the nuclear relaxation time  $T_1$ . When the nuclear relaxation occurs by a magnetic origin, the relaxation time  $T_1$  is expressed in terms of the electron-spin correlation function as

$$\frac{1}{T_1} = \frac{(\gamma_n A)^2}{2} \int_{-\infty}^{\infty} dt \langle \sigma_+(t, \mathbf{x}) \sigma_-(0, \mathbf{x}) \rangle e^{-i\omega_0 t}, \quad (3.1)$$

where  $\gamma_n$  is the nuclear gyromagnetic ratio and  $A$  the hyperfine coupling constant, and  $\omega_0$  the resonance frequency. In the TFD Eq. (3.1) can be expressed in terms of the spectral function of the spin-fluctuation Green's

function  $D(\omega_0, \mathbf{q})$  as follows:

$$\frac{1}{T_1} = \pi(\gamma_n A)^2 \sum_{\mathbf{q}} D(\omega_0, \mathbf{q}) \frac{e^{\omega_0/T}}{e^{\omega_0/T} - 1}, \quad (3.2)$$

$$\approx \pi(\gamma_n A)^2 T \sum_{\mathbf{q}} \frac{D(\omega_0, \mathbf{q})}{\omega_0}. \quad (3.3)$$

We now calculate the spin-fluctuation Green's function  $\chi^{ab}(q)$  to obtain  $D(\omega_0, q)$ . Let us consider a three-point function

$$\langle O(\beta) | T \sigma_{\frac{z}{2}}^{\alpha}(x) \Psi^{\beta}(y) \Psi^{\gamma}(z) | O(\beta) \rangle = \left[ \frac{i}{(2\pi)^4} \right]^2 \int d^4 p d^4 q \left[ -\varepsilon^{\alpha} S^{\alpha\beta}(p) \tau_2 {}^t S^{\gamma\alpha}(-p-q) \tau_2 \right. \\ \left. + i \sum_{\xi, \eta} \chi^{\alpha\xi}(q) S^{\beta\eta}(p) \Gamma_{\frac{z}{2}}^{\xi\eta\zeta}(p; -p-q) {}^t S^{\gamma\zeta}(-p-q) \right] e^{ipy+iqx-i(p+q)z}, \quad (3.4)$$

where the vertex function  $\Gamma_{\frac{z}{2}}^{\xi\eta\zeta}(p; -p-q)$  was introduced to express the proper part of the three-point function.<sup>25</sup> The graphical representation of Eq. (3.4) is given in Fig. 3(a). The equation for  $\chi^{ab}(q)$  can be obtained from Eq. (3.4) by taking the limit of  $z \rightarrow y$  as

$$\chi^{ab}(x-y) = \langle O(\beta) | T \sigma_{\frac{z}{2}}^{\alpha}(x) \sigma_{\frac{z}{2}}^{\beta}(y) | O(\beta) \rangle = -\frac{1}{2} \sum_{a,b} \langle O(\beta) | T \sigma_{\frac{z}{2}}^{\alpha}(x) \Psi_a^{\beta}(y) \Psi_b^{\beta}(y) | O(\beta) \rangle \tau_2^{ab} \varepsilon^{\beta} \\ = \left[ \frac{i}{(2\pi)^4} \right]^2 \int d^4 q d^4 p \left[ -\frac{1}{2} \varepsilon^{\alpha} T_r [S^{\alpha\beta}(p) \tau_2 {}^t S^{\beta\alpha}(-p-q)] \varepsilon^{\beta} \right. \\ \left. + \frac{1}{2} \sum_{\xi, \eta, \zeta} \chi^{\alpha\xi}(q) T_r [S^{\beta\eta}(p) \Gamma_{\frac{z}{2}}^{\xi\eta\zeta}(p; -p-q) {}^t S^{\beta\zeta}(-p-q) \tau_2] \varepsilon^{\beta} \right] e^{iq(x-y)}. \quad (3.5)$$

Thus, we have the equation

$$\chi^{ab}(q) = \left[ \frac{i}{(2\pi)^4} \right] \int d^4 p \left[ \frac{1}{2} \varepsilon^{\alpha} T_r [S^{\beta\alpha}(p) \tau_2 {}^t S^{\beta\alpha}(-p-q) \tau_2] \varepsilon^{\beta} \right. \\ \left. - \frac{1}{2} \sum_{\xi, \eta, \zeta} \chi^{\alpha\xi}(q) T_r [S^{\beta\eta}(p) \Gamma_{\frac{z}{2}}^{\xi\eta\zeta}(p; -p-q) {}^t S^{\beta\zeta}(-p-q) \tau_2] \varepsilon^{\beta} \right]. \quad (3.6)$$

Here we use the relation  ${}^t \tau_2 = -\tau_2$ . If the Hartree Green's function is used for  $S^{ab}(p)$  and the vertex function is approximated as  $\Gamma_{\frac{z}{2}}^{\xi\eta\zeta}(p; -p-q) \approx U \delta^{\eta\xi} \delta^{\zeta\xi} \tau_2$ , Eq. (3.6) is reduced to that in the random-phase approximation (RPA). To solve Eq. (3.6) in an approximation beyond the RPA we approximate the vertex function in the following form:

$$\Gamma_{\frac{z}{2}}^{\xi\eta\zeta}(p; -p-q) = \Theta^{\eta\xi}(p) \Theta^{\zeta\xi}(-p-q) \tau_2. \quad (3.7)$$

Here, the function  $\Theta^{ab}(p)$  is assumed to have the same spectral representation as that of a fermion Green's function. By this assumption  $\chi^{ab}(q)$  obtained from Eq. (3.6) is insured to have the bosonlike spectral representation as seen in the following. Substituting Eq. (3.7) into Eq. (3.6) and introducing  $\tilde{S}^{ab}(p)$  by

$$\tilde{S}^{ab}(p) = \sum_{\gamma} S^{a\gamma}(p) \Theta^{\gamma\beta}(p), \quad (3.8)$$

we obtain

$$\chi^{ab}(q) = K^{ab}(q) - \sum_{\xi} \chi^{\alpha\xi}(q) \varepsilon^{\xi} L^{\xi\beta}(q), \quad (3.9)$$

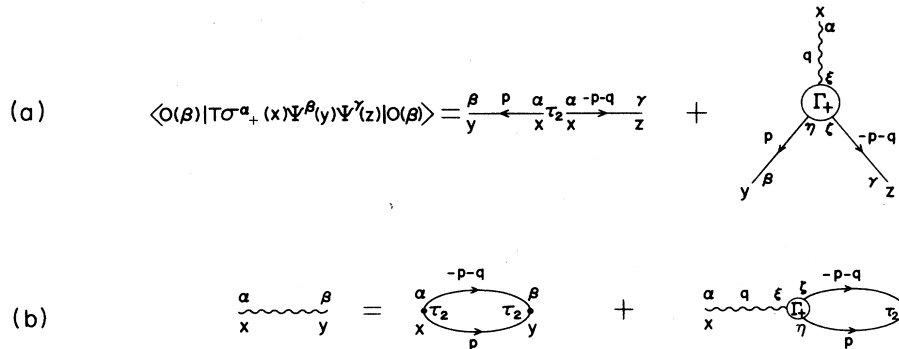


FIG. 3. Graphical representation for (a) the three-point function  $\langle \sigma_{\frac{z}{2}}^{\alpha}(x) \Psi^{\beta}(y) \Psi^{\gamma}(z) \rangle$  and (b) the equation for the spin-fluctuation Green's function  $\chi^{ab}(x-y)$ .



where

$$K^{a\beta}(q) = \frac{i}{(2\pi)^4} \int d^4p \frac{1}{2} \varepsilon^a T_r [S^{\beta a}(p) \tau_2 {}^t S^{\beta a}(-p-q) \tau_2] \varepsilon^\beta, \quad (3.10)$$

$$L^{a\beta}(q) = \frac{i}{(2\pi)^4} \int d^4p \frac{1}{2} \varepsilon^a T_r [\tilde{S}^{\beta a}(p) \tau_2 {}^t \tilde{S}^{\beta a}(-p-q) \tau_2] \varepsilon^\beta. \quad (3.11)$$

The functions  $K^{a\beta}(q)$  and  $L^{a\beta}(q)$  can be separated into their real and imaginary parts as follows:

$$K^{a\beta}(q) = K_1(q) \varepsilon^a \delta^{a\beta} - i K_2(q) [U_B(q_0) U_B(q_0)^\dagger]^{a\beta}, \quad (3.12)$$

$$L^{a\beta}(q) = L_1(q) \varepsilon^a \delta^{a\beta} - i L_2(q) [U_B(q_0) U_B(q_0)^\dagger]^{a\beta}, \quad (3.13)$$

where

$$K_1(q) = \frac{1}{\pi} \int dv \frac{1}{q_0 - v} K_2(v, \mathbf{q}), \quad (3.14)$$

$$K_2(q) = \pi \int \frac{d^4p}{(2\pi)^4} \frac{1}{2} T_r [\rho(p_0, \mathbf{p}) \tau_2 \rho(-p_0 - q_0, -\mathbf{p} - \mathbf{q}) \tau_2] [f_F(p_0) - f_F(p_0 + q_0)], \quad (3.15)$$

$$L_1(q) = \frac{1}{\pi} \int dv \frac{1}{q_0 - v} L_2(v, \mathbf{q}), \quad (3.16)$$

$$L_2(q) = \pi \int \frac{d^4p}{(2\pi)^4} \frac{1}{2} T_r [\tilde{\rho}(p_0, \mathbf{p}) \tau_2 \rho(-p_0 - q_0, -\mathbf{p} - \mathbf{q}) \tau_2] [f_F(p_0) - f_F(p_0 + q_0)], \quad (3.17)$$

$$U_B(q_0) = \begin{vmatrix} c_B(q_0) & d_B(q_0) \\ d_B(q_0) & c_B(q_0) \end{vmatrix}. \quad (3.18)$$

with

$$c_B^2(q_0) = \frac{e^{q_0/T}}{e^{q_0/T} - 1}, \quad d_B^2(q_0) = \frac{1}{e^{q_0/T} - 1}. \quad (3.19)$$

In Eq. (3.17)  $\tilde{\rho}(p_0, \mathbf{p})$  is the spectral function of  $\tilde{S}^{a\beta}(p)$ . Thus substitution of Eqs. (3.12) and (3.13) into Eq. (3.9) gives the following spectral function of the spin-fluctuation Green's function:

$$D(q) = \frac{1}{\pi} \frac{K_2(q) + K_2(q)L_1(q) - K_1(q)L_2(q)}{[1 + L_1(q)]^2 [L_2(q)]^2}. \quad (3.20)$$

Let us now investigate the vertex function (3.7) to obtain the functions  $L_1(q)$  and  $L_2(q)$  in Eq. (3.20). As seen later renormalization of the vertex function leads to a strong temperature dependence in the superconducting state. In the following we present a renormalization scheme for  $\Gamma_{\ddagger}^{a\beta\gamma}(p; -p-q)$  by using the Ward-Takahashi (WT) relation which stems from the spin-rotational invariance of the system.

Consider the WT relation<sup>26</sup>

$$\tau_2 [\Xi^{a\beta}(-p) + \Pi^{a\beta}(-p)] + [\Xi^{a\beta}(p) + \Pi^{a\beta}(p)] \tau_2 = h \sum_{\gamma, \delta} \varepsilon^\gamma \chi^{\gamma\delta}(0) \Gamma_{\ddagger}^{a\beta}(p; -p) \quad (3.21)$$

$$= h \chi(0) \sum_{\gamma} \Gamma_{\ddagger}^{a\beta}(p; -p), \quad (3.22)$$

where  $h$  is an external magnetic field acting on the electron spin. The derivation of the WT relation (3.21) is given in Appendix A. In deriving (3.22) from (3.21) we used the fact that  $\chi^{\gamma\delta}(0)$  is real and  $\chi^{\gamma\delta}(0) = \chi(0) \varepsilon^\gamma \delta^{\gamma\delta}$ . Since the WT relation gives a relation between the self-energy functions and the vertex function  $\Gamma_{\ddagger}^{a\beta}(p; -p)$  we can make use of this relation to obtain the vertex function

from the self-energy function obtained in Sec. II. Let us first consider the Hartree term (2.23). In the presence of a weak magnetic field  $h$ ,  $\Pi_{\text{Hartree}}$  is rewritten in the form

$$\Pi_{\text{Hartree}}^{a\beta}(p) = U n_0 \delta^{a\beta} \tau_3 + \frac{1}{2} U h \chi(0) \delta^{a\beta} + \tilde{\Delta}_0 \delta^{a\beta} \tau_1, \quad (3.23)$$

where  $n_0$  is the electron density per spin in the absence of  $h$ . If  $\Pi_{\text{Hartree}}$  is substituted into the self-energy function in Eq. (3.21) and  $\Xi^{a\beta}(p)$  is neglected, the vertex function

$$\Gamma_{\ddagger}^{a\beta}(p; -p) = U \delta^{a\beta} \delta^{\beta\delta} \tau_2 \quad (3.24)$$

is obtained from the WT relation (3.22). This is nothing but the vertex function in the RPA. This result indicates that the RPA for the susceptibility is consistent with the Hartree approximation for the one-electron Green's function. The one-loop correction to the self-energy function [the second term on the right-hand side of Eq. (2.22)] leads to a correction to the RPA vertex function (3.24). When the self-energy function (2.22) is substituted into the WT relation and the vertex function is renormalized at  $p = p_F \equiv (0, \mathbf{p}_F)$  and  $T = T_c$  as

$$\text{Re} \Gamma_{\ddagger}^{a\beta}(p_F; -p_F) \Big|_{T=T_c} = U_r \delta^{a\beta} \delta^{\beta\delta} \tau_2, \quad (3.25)$$

where  $U_r$  is the renormalized coupling constant introduced in Sec. II, we obtain the function  $\Theta^{a\delta}(p)$  defined by Eq. (3.7) as follows:

$$\Theta^{a\delta}(p) = \Theta_1(p) \delta^{a\delta} - i \pi \theta(p) [U_F(p_0) \hat{e} U_F(p_0)^\dagger]^{a\delta}, \quad (3.26)$$

where

$$\Theta_1(p) = \sqrt{\Lambda_r(p)}, \quad (3.27)$$

$$\theta(p) = - \int d\omega \frac{1}{p_0 - \omega} \sqrt{\Lambda_r(\omega, \mathbf{p})}, \quad (3.28)$$

with

$$\Lambda_r(p) = U_r + \left( \frac{1}{\chi(0)} \frac{\partial}{\partial p_0} \int d\omega \frac{1}{p_0 - \omega} \Omega_0(\omega, \mathbf{p}_F) \right)_{p_0=0, T=T_c} - \frac{1}{\chi(0)} \frac{\partial}{\partial p_0} \int d\omega \frac{1}{p_0 - \omega} \Omega_0(\omega, \mathbf{p}). \quad (3.29)$$

Here,  $\Omega_0(\omega, \mathbf{p})$  is given by Eq. (2.30). The details of the above renormalization procedure is presented in Appendix B.

Let us now calculate the longitudinal nuclear relaxation time  $T_1$ . From Eqs. (3.3) and (3.20) we have

$$\frac{1}{T_1} = (\gamma_n A)^2 T \sum_{\mathbf{q}} \frac{K_2(\omega_0, \mathbf{q}) + K_2(\omega_0, \mathbf{q})L_1(\omega_0, \mathbf{q}) - K_1(\omega_0, \mathbf{q})L_2(\omega_0, \mathbf{q})}{\{[1 + L_1(\omega_0, \mathbf{q})]^2 + [L_2(\omega_0, \mathbf{q})]^2\} \omega_0}. \quad (3.30)$$

Since  $\omega_0$  is quite small, we take the limit  $\omega_0 \rightarrow 0$ . Noting

$$K_2(\omega_0, \mathbf{q}) \approx \frac{\pi \omega_0}{T} \int \frac{d^4 p}{(2\pi)^3} \frac{1}{2} T_r [\rho(p_0, \mathbf{p}) \tau_2 \rho(-p_0, -\mathbf{p} - \mathbf{q}) \tau_2] \frac{e^{p_0/T}}{(e^{p_0/T} + 1)^2} \quad (3.31)$$

$$\equiv \frac{\pi \omega_0}{T} K_2(\mathbf{q}), \quad (3.32)$$

$$L_2(\omega_0, \mathbf{q}) \approx \frac{\pi \omega_0}{T} \int \frac{d^4 p}{(2\pi)^3} \frac{1}{2} T_r [\tilde{\rho}(p_0, \mathbf{p}) \tau_2 \tilde{\rho}(-p_0, -\mathbf{p} - \mathbf{q}) \tau_2] \frac{e^{p_0/T}}{(e^{p_0/T} + 1)^2} \quad (3.33)$$

$$\equiv \frac{\pi \omega_0}{T} L_2(\mathbf{q}), \quad (3.34)$$

from Eqs. (3.15) and (3.17), we have

$$\frac{1}{T_1} = \pi (\gamma_n A)^2 \sum_{\mathbf{q}} \frac{K_2(\mathbf{q}) + K_2(\mathbf{q})L_1(\mathbf{q}) - K_1(\mathbf{q})L_2(\mathbf{q})}{[1 + L_1(\mathbf{q})]^2}, \quad (3.35)$$

where

$$L_1(\mathbf{q}) = L_1(0, \mathbf{q}), \quad K_1(\mathbf{q}) = K_1(0, \mathbf{q}). \quad (3.36)$$

To simplify the numerical calculation we make a further approximation to Eq. (3.35). Since in the numerator of Eq. (3.35)

$$|K_2(\mathbf{q})L_1(\mathbf{q}) - K_1(\mathbf{q})L_2(\mathbf{q})| \ll K_2(\mathbf{q}), \quad (3.37)$$

we approximate Eq. (3.35) by

$$\frac{1}{T_1} \approx \pi (\gamma_n A)^2 \sum_{\mathbf{q}} \frac{K_2(\mathbf{q})}{[1 + L_1(\mathbf{q})]^2}. \quad (3.38)$$

Furthermore, we approximate Eq. (3.38) as

$$\begin{aligned} \frac{1}{T_1} &\approx \pi (\gamma_n A)^2 \left\langle \frac{1}{[1 + L_1(q)]^2} \right\rangle \int dp_0 \\ &\quad \times \frac{1}{2} T_r \left[ \sum_{\mathbf{p}} \rho(p_0, \mathbf{p}) \tau_2 \sum_{\mathbf{p}'} \rho(-p_0, \mathbf{p}') \right] \frac{e^{p_0/T}}{e^{p_0/T} + 1}, \end{aligned} \quad (3.39)$$

where

$$\left\langle \frac{1}{[1 + L_1(q)]^2} \right\rangle = \frac{1}{V_q} \int \frac{d^3 q}{(2\pi)^3} \frac{1}{[1 + L_1(q)]^2}. \quad (3.40)$$

Here, the integration by  $\mathbf{q}$  is performed within the sphere with the radius of a cutoff momentum  $q_c$ , i.e.,

$$\left\langle \frac{1}{[1 + L_1(q)]^2} \right\rangle = \frac{3}{8\pi^3 q_c^3} \int^{q_c} dq \frac{q^2}{[1 + L_1(q)]^2}. \quad (3.41)$$

The value of  $q_c$  is chosen as  $q_c \xi_0 = 5$  in the following numerical calculations, where  $\xi_0$  is the superconducting coherence length at  $T=0$  K. Substituting the spectral function (2.38) into Eq. (3.39) and assuming particle-hole symmetry, we finally obtain the following result for  $T_1$ .

$$\frac{1}{T_1} = \pi (\gamma_n A)^2 \left\langle \frac{1}{[1 + L_1(\mathbf{q})]^2} \right\rangle \int dp_0 [N_s^{(0)}(p_0)^2 + N_s^{(1)}(p_0)^2] \frac{e^{p_0/T}}{(e^{p_0/T} + 1)^2}, \quad (3.42)$$

where

$$N_s^{(0)}(p_0) = N(0) \left[ \Omega_p^{(0)} \left( \frac{(\alpha_p^2 + \beta_p^2)^{1/2} - \alpha_p}{2(\alpha_p^2 + \beta_p^2)} \right)^{1/2} + p_0 \left( \frac{(\alpha_p^2 + \beta_p^2)^{1/2} + \alpha_p}{2(\alpha_p^2 + \beta_p^2)} \right)^{1/2} \right], \quad (3.43)$$

$$N_s^{(1)}(p_0) = N(0) \left[ -\Omega_p^{(0)} \left( \frac{(\alpha_p^2 + \beta_p^2)^{1/2} - \alpha_p}{2(\alpha_p^2 + \beta_p^2)} \right)^{1/2} + p_0 \left( \frac{(\alpha_p^2 + \beta_p^2)^{1/2} + \alpha_p}{2(\alpha_p^2 + \beta_p^2)} \right)^{1/2} \right], \quad (3.44)$$

Here  $\alpha_p$  and  $\beta_p$  are given in Eqs. (2.44) and (2.45).

### B. Numerical results

In Fig. 4 the numerical results for the temperature dependence of  $1/T_1$  are plotted for various values of the normalized coupling constant  $U_r N(0)$ ,  $N(0)$  being the density of states at the Fermi level in the normal state. When the value of  $U_r N(0)$  is small, a hump is observed just below  $T_c$  as in the usual BCS theory [Fig. 4(a)]. This hump originates from a sharp peak of the density of states above the energy gap (Fig. 2). As the value of  $U_r N(0)$  increases, the hump gradually shrinks and finally disappears. As seen in Fig. 4(b), when  $U_r N(0)$  further increases,  $1/T_1$  has an extremely sharp drop just below  $T_c$ .

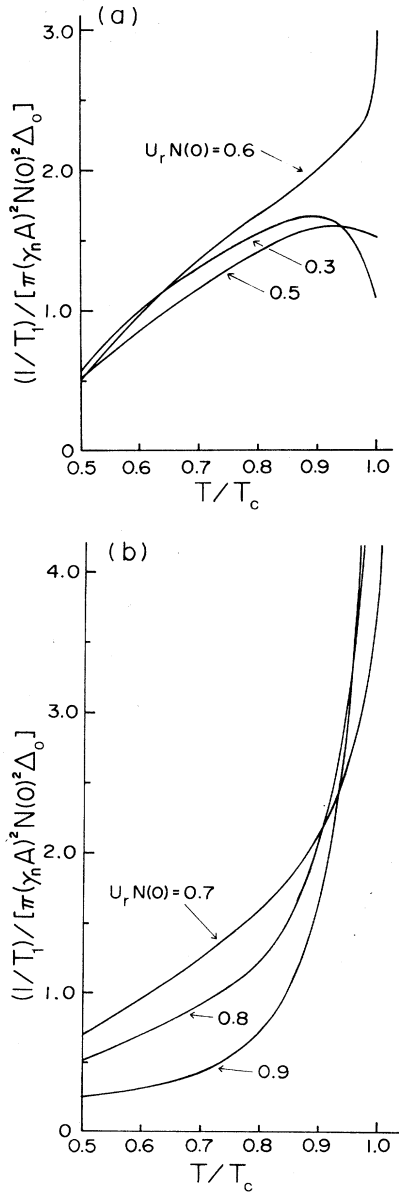


FIG. 4. Temperature dependence of  $1/T_1$  in the superconducting state for the parameter values, (a)  $U_r N(0) = 0.3, 0.5,$  and  $0.6,$  and (b)  $U_r N(0) = 0.7, 0.8,$  and  $0.9.$

To see the origin of the temperature dependence of  $1/T_1$  mentioned above, we first examine the contribution from the "bubble diagram," i.e., the integral on the right-hand side of Eq. (3.42),

$$\int dp_0 [N_s^{(0)}(p_0)^2 + N_s^{(1)}(p_0)] e^{p_0/T} / (e^{p_0/T} + 1)^2. \quad (3.45)$$

As can easily be seen, this function is reduced to the BCS expression for  $1/T_1$  in the limit of  $U \rightarrow 0$ , i.e.,  $\Omega_p^{(0)}, \Omega_p^{(1)} \rightarrow 0$ :

$$2 \int dp_0 \frac{p_0^2}{p_0^2 - \Delta_p^2} [1 + (\Delta_p/E_p)^2] e^{p_0/T} / (e^{p_0/T} + 1)^2, \quad (3.46)$$

Therefore, the function (3.45) has a hump structure as seen in the curve for  $U_r N(0) = 0.3$  in Fig. 5, as  $1/T_1$  of the BCS theory has. On the other hand, the function for  $U_r N(0) = 0.9$  has a monotonic decrease with decreasing temperature, as seen in Fig. 5. This monotonic decrease comes from the fact that the density of states has no peak structure in the gapless region near  $T_c$ . Thus, the disappearance of the hump in the  $1/T_1$  is understood to come from the gapless nature of the superconductivity due to the strong correlation. The sharp drop of  $1/T_1$  just below  $T_c$  for large  $U_r N(0)$  is caused by the enhancement factor in front of the integral in Eq. (3.42),

$$\left\langle \frac{1}{[1 + L_1(q)]^2} \right\rangle \quad (3.47)$$

as seen in the following. This factor has a large value in the normal state, yielding the large value of  $1/T_1$  as observed in the experiments. In the superconducting state this factor rapidly decreases with decreasing temperature when  $U_r$  is large. This temperature dependence comes from that  $L_1(q)$  is negative and its magnitude rapidly decreases in the superconducting state. This fact is easily seen in the weak-coupling case because  $L_1(q)$  is proportional to the irreducible spin susceptibility of the superconducting electrons. The temperature dependence of the renormalized vertex function  $\Lambda_r(p)$  is also important for the temperature dependence of  $L_1(q)$ . In Fig. 6 we present the numerical results for  $\Lambda_r(0, p_F)$ . As seen in this

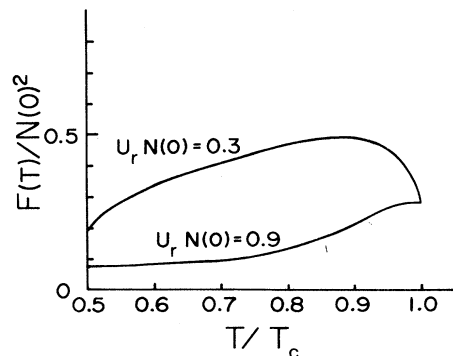


FIG. 5. Temperature dependence of the "bubble diagram."

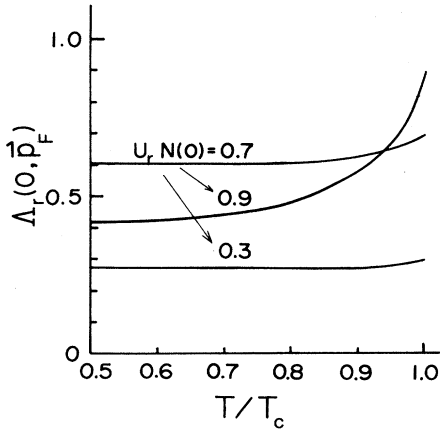


FIG. 6. Temperature dependence of the renormalized vertex function  $\Lambda_r(0, \vec{p}_F)$ .

figure,  $\Lambda_r(0, \vec{p}_F)$  has a strong temperature dependence and its value is much reduced in the superconducting state for large  $U_r$ . This dependence comes from the temperature dependence of the last term on the right-hand side of (3.29). This term increases with decreasing temperature because the absolute value of the spin susceptibility  $\chi(0)$  decreases as superconductivity develops. As seen from Eq. (2.30), the term is on the order of  $U_r^2$ . Therefore, in the case of large  $U_r$ , the strong renormalization of the vertex function occurs. Physically, this renormalization effect for the vertex function in the superconducting state can be understood in the following way. The number of the low-energy excited states in the one-electron channel decreases as the energy gap develops with decreasing temperature in the superconducting state. This causes a decrease in the probability that the low-energy spin fluctuations scatter the electrons. In the case of large  $U_r$ , the spectral density of the spin fluctuations is large at low energies. Therefore, the renormalization effect at low energies is stronger in the strong correlation case.

The above numerical results were obtained using the ferromagnetic spin fluctuations for the spin-fluctuation Green's function. The similar temperature dependence of the enhancement factor (3.47) is also expected in the system with antiferromagnetic spin fluctuations in the strong-coupling case as discussed below. Roughly speaking, the temperature dependence of  $L_1(\mathbf{q})$  is given by the product of the "bubble diagram" corresponding to a single-particle, hole pair excitation and the vertex function  $\Gamma_{\vec{q};\beta\gamma}^{\xi;\eta\alpha}(p; -p - Q)$ . Although the "bubble diagram" with a wave number much larger than the inverse superconducting coherence length is not affected by the onset of superconductivity, the sharp decrease of the enhancement factor just below  $T_c$  is expected to arise from the temperature dependence of the vertex function in the system with large antiferromagnetic spin fluctuations in the following way. The equation for the vertex function  $\Gamma_{\vec{q};\beta\gamma}^{\xi;\eta\alpha}(p; -p - q)$  can be expressed as shown graphically in Fig. 7 in terms of a new vertex function  $\Gamma_{\vec{q};\beta\gamma}^{\xi;\eta\alpha}(p, p + Q - q; q, Q)$ .<sup>27</sup> This vertex function describes the process that the spin fluctuations decay into an electron, hole pair and other

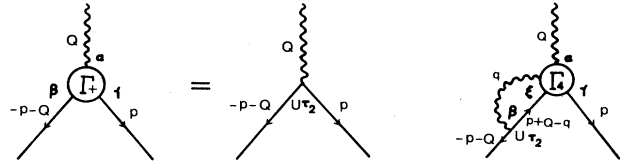


FIG. 7. Graphical representation of the equation for the vertex function  $\Gamma_{\vec{q};\beta\gamma}^{\xi;\eta\alpha}(-p - q; p)$ .

spin fluctuations. Let us consider the case that the wave number  $Q$  in the second term in Fig. 7 is close to the zone boundary (the wave number of the antiferromagnetic spin fluctuations). When the wave number  $q$  of the internal spin fluctuations is close to the zone boundary and  $q \approx Q$ ,  $\Gamma_{\vec{q};\beta\gamma}^{\xi;\eta\alpha}$  is expected to be small because the scattering between the particle and hole pair is almost a forward scattering and, thus, this process is suppressed in the superconducting state. Hence, a large contribution to the vertex function comes mainly from the scattering process with small  $q$ . As given in Ref. 27, a study of the WT relation originating from the spin-rotational invariance shows that the vertex function  $\Gamma_{\vec{q};\beta\gamma}^{\xi;\eta\alpha}(p, p + Q; 0, Q)$  carries a factor  $1/\chi(0)$  in the paramagnetic state. Since  $|1/\chi(0)|$  increases the superconducting order parameter develops, this process is expected to give a strong renormalization of the vertex function  $\Gamma_{\vec{q};\beta\gamma}^{\xi;\eta\alpha}(p; -p - q)$  even for the antiferromagnetic spin fluctuations in the superconducting state. Therefore, we may expect the sharp decrease of the enhancement factor even in the system in which antiferromagnetic spin fluctuations dominate. The calculation of  $1/T_1$  in this system is now in progress.

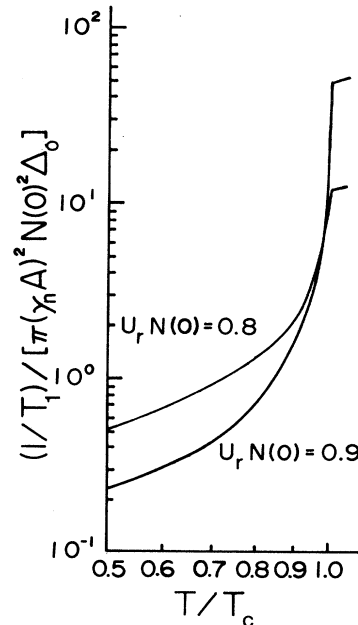


FIG. 8. Temperature dependence of  $1/T_1$  in a log scale.

#### IV. COMPARISON WITH THE EXPERIMENTS

In this paper we investigated the effects of the spin fluctuations on the superconducting state and calculated the nuclear relaxation time  $T_1$ . In the case of large  $U$ , the large lifetime effect arises from the self-energy correction due to the spin fluctuations, bringing a gapless superconducting state near  $T_c$ . As a result the hump of  $1/T_1$  which is usually observed in BCS superconductors disappears and the inverse relaxation time  $1/T_1$  monotonically decreases with decreasing temperature below  $T_c$ . The decrease just below  $T_c$  is extremely sharp. This sharp decrease comes from the fact that the enhancement factor of the electron-spin susceptibility rapidly decreases as the superconductivity develops. Especially, the renormalization effect for the spin-fluctuation vertex function plays an important role for the drastic decrease of the enhancement factor. The importance of spin fluctuations to the nuclear relaxation of Cu has also been pointed out by Imai *et al.*<sup>17</sup>

Let us now discuss the experimental results for  $1/T_1$  of Cu II in  $\text{YBa}_2\text{Cu}_3\text{O}_{7-y}$  in the light of the calculated results. As mentioned in the Introduction, the  $1/T_1$  vs  $T$  curve for Cu II shows no hump and a sharp decrease just below  $T_c$ . The value of  $1/T_1$  is much larger than the value estimated from the Korringa relation. To compare with experimental results which are usually plotted on a log scale, we plot the logarithm of the values of  $1/T_1$  and  $T$  in the case of  $U_r N(0) = 0.8$  and  $0.9$  in Fig. 8. As seen in Fig. 8, the curve shows no hump below  $T_c$ . When temperature decreases from  $T_c$ , the curve sharply descends near  $T_c$  and tends to the BCS value at low temperatures. This temperature dependence is in good agreement with the experiments of NQR of Cu II in  $\text{YBa}_2\text{Cu}_3\text{O}_{7-y}$ .<sup>14-17</sup> It is noted that the observed uniform susceptibility in  $\text{YBa}_2\text{Cu}_3\text{O}_{7-y}$  is not much enhanced compared with the value of the Pauli paramagnetic susceptibility.<sup>8,28</sup> This fact indicates that the enhancement of  $1/T_1$  in the normal state is caused by the antiferromagnetic spin fluctuations. Their wave number are about  $(4 \text{ \AA})^{-1}$ . The superconducting coherence length  $\xi_0$  is about  $20 \text{ \AA}$  in the  $ab$  plane and  $2-4 \text{ \AA}$  along the  $c$  axis. Hence, the simple RPA calculation cannot account for a sharp decrease in the temperature dependence of  $1/T_1$  just below  $T_c$ . It is essential to take account of the strong temperature dependence of the spin-fluctuation vertex function.

In the present theory the Knight shift is proportional to  $K_1(0)/[1+L_1(0)]$   $K_1(0)$  and  $L_1(0)$  being given by (3.36). Since the enhancement factor  $1/[1+L_1(0)]$  is drastically reduced in the superconducting state, we predict a much steeper decrease of the Knight shift below  $T_c$  than that expected from the BCS theory. Actually, the very steep decrease of the Knight shift of Cu II has been observed in the superconducting state of  $\text{YBa}_2\text{Cu}_3\text{O}_{7-y}$  by Kitaoka, Hiramatsu, Kondo, and Asayama.<sup>16</sup>

The gapless superconducting state appears only near  $T_c$  and the superconducting state with the energy gap remains at low temperatures. Therefore, the present theoretical result is consistent with the experimental results of tunneling and optical measurements in which the clear energy gaps have been observed at low temperatures.<sup>10</sup>

As seen in the present paper, the anomalous behavior of the nuclear relaxation observed in  $\text{YBa}_2\text{Cu}_3\text{O}_{7-y}$  is explained on the basis of the BCS pairing if the strong correlation effect is taken into account. Consequently, we conclude that together with other experimental results of the oxide superconductors the BCS type pairing is still responsible for the high- $T_c$  superconductivity even in the oxides. However, for the origin of the large binding energy accountable for the high transition temperature we may need some other mechanism than the phonon mechanism.

#### ACKNOWLEDGMENTS

The authors would like to thank Professor Y. Muto, Dr. Takahashi, and Mr. N. Takezawa for helpful discussions. This work was supported by a Grant-in-Aid from the Ministry of Education, Science and Culture, Japan, and High Field Laboratory for Superconducting Materials, Tohoku University.

#### APPENDIX A

The WT relation at finite temperatures (3.21) can be easily obtained by extending the derivation at  $T=0$  K, so that we derive the WT relation at  $T=0$  K in this appendix.

Consider the generating functional of the Green's function.

$$W(\eta, \eta^\dagger) = \frac{1}{N} \int (d\psi_\sigma d\psi_\sigma^\dagger) \exp \left[ i \int d^4x [L(x) + \frac{1}{2} h \sigma_3(x) + \eta_\sigma^\dagger(x) \psi_\sigma(x) + \psi_\sigma^\dagger(x) \eta_\sigma(x)] \right], \quad (\text{A1})$$

where  $\eta_\sigma(x)$  and  $\eta_\sigma^\dagger(x)$  are the source fields,  $L(x)$  is the Lagrangian density of our system and is assumed invariant under the spin rotation,  $\psi \rightarrow \exp(i\theta\sigma_i)\psi$ , and  $\sigma_3(x)$  and  $N$  are defined by

$$\sigma_3(x) = \psi_1^\dagger(x) \psi_1 - \psi_2^\dagger(x) \psi_2, \quad (\text{A2})$$

$$N = \int (d\psi_\sigma d\psi_\sigma^\dagger) \exp \left[ i \int d^4x [L(x) + \frac{1}{2} h \sigma_3(x)] \right]. \quad (\text{A3})$$

For an infinitesimal spin rotation

$$\psi(x) \rightarrow \psi(x) + i\theta\sigma_i\psi(x), \quad (\text{A4})$$

the variation of the generating functional (A1) is given by

$$\delta W[\eta, \eta^\dagger] = i \int d^4x \theta \left( \frac{1}{2} h \psi^\dagger(x) (\sigma_3, \sigma_i) \psi(x) + [\eta^\dagger(x) \sigma_i \psi(x) - \psi^\dagger(x) \sigma_i \eta(x)] \right)_{\eta, \eta^\dagger}, \quad (\text{A5})$$

where

$$\langle \cdots \rangle_{\eta, \eta^\dagger} = \frac{1}{N} \int (d\psi_\sigma d\psi_\sigma^\dagger) (\cdots) \exp \left[ i \int d^4x [L(x) + \frac{1}{2} h \sigma_3(x) + \eta_\sigma^\dagger(x) \psi_\sigma(x) + \psi_\sigma^\dagger(x) \eta_\sigma(x)] \right]. \quad (\text{A6})$$

Since the transformation (A4) is only a change of integration variables in the functional integral (A1), the variation (A5) should vanish. Thus, in the case of  $\sigma_i = \sigma_+$ , Eq. (A5) leads to the relation

$$\int d^4x \langle \eta_1^\dagger(x) \psi_1(x) - \psi_1^\dagger(x) \eta_1(x) + h \sigma_+(x) \rangle_{\eta, \eta^\dagger} = 0. \quad (\text{A7})$$

In the Nambu representation Eq. (A7) is expressed as

$$\int d^4x \langle \eta_1^\dagger(x) \psi_2^\dagger(x) - \psi_1^\dagger(x) \eta_2^\dagger(x) + h \sigma_+(x) \rangle_{\eta, \eta^\dagger} = 0. \quad (\text{A8})$$

Operating  $\delta^2/\delta_d^\dagger(x_1) \delta \eta_b^\dagger(x_2)$  on Eq. (A8) and taking the limit of  $\eta, \eta^\dagger \rightarrow 0$ , we can derive the relation

$$\tau_3 S(x_1 - x_2) \tau_1 - \tau_1^\dagger S(x_2 - x_1) \tau_3 = -i \int d^4x \tau_3 \langle 0 | T \sigma_+(x) \Psi(x_1) \Psi^\dagger(x_2) | 0(\beta) \rangle \tau_3. \quad (\text{A9})$$

We define the Fourier transformation of the three-point function as

$$\langle 0 | T \sigma_+(x) \Psi(x_1) \Psi^\dagger(x_2) | 0 \rangle = [i/(2\pi)^4] \int d^4p d^4q [-iS(p) \tau_2^\dagger S(-p-q) + i\chi(q) S(p) \Gamma_+(p; -p-q)^\dagger S(-p-q)] e^{ipx_1 + iqx - i(p+q)x_2}, \quad (\text{A10})$$

Substituting Eq. (A10) into Eq. (A9), we obtain

$$\tau_2^\dagger S^{-1}(-p) + S^{-1}(p) \tau_2 = h \tau_2 - h \chi(0) \Gamma_+(p; -p). \quad (\text{A11})$$

Since  $S^{-1}(p)$  is written in the form

$$S^{-1}(p) = (p_0 + \frac{1}{2}) - \varepsilon_p \tau_3 - \Xi(p) - \Pi(p), \quad (\text{A12})$$

Eq. (A11) gives the WT relation at  $T=0$  K,

$$\tau_2 [\Xi(-p) + \Pi(-p)] + [\Xi(p) + \Pi(p)] \tau_2 = h \chi(0) \Gamma_+(p; -p). \quad (\text{A13})$$

## APPENDIX B

In this appendix we derive the renormalized vertex function (3.29). We assume that the real part of the vertex function  $\Gamma_{\xi_i \eta_i}^{\xi_i \eta_i}(p; -p)$  takes the form

$$\text{Re} \Gamma_{\xi_i \eta_i}^{\xi_i \eta_i}(p; -p) = \Lambda(p) \sigma^{\eta_i \xi_i} \delta^{\xi_i \xi_i} \tau_2, \quad (\text{B1})$$

and the magnetic field dependence of  $\Xi^{ab}(p)$  is negligible. In this case the WT relation (3.22) becomes

$$\text{Re} [\tau_2 \Pi^{ab}(-p) + \Pi^{ab}(p) \tau_2] = h \chi(0) \Lambda(p) \delta^{ab} \tau_2. \quad (\text{B2})$$

This equation gives the following relation between the  $\tau_0$  component of  $\Pi^{ab}(p)$  and  $\Lambda(p)$ :

$$\Lambda(p) = U + \frac{1}{h \chi(0)} \int d\omega \left[ \frac{1}{p_0 - \omega} + \frac{1}{-p_0 - \omega} \right] \Omega_0(\omega, \mathbf{p}; h), \quad (\text{B3})$$

where  $\Omega_0(\omega, \mathbf{p}; h)$  is the spectral function of the self-energy function along  $\tau_0$  direction in the presence of  $h$ . Since we have the relation

$$\Omega_0(\omega, \mathbf{p}; h) = \Omega_0(\omega - \frac{1}{2} h, \mathbf{p}), \quad (\text{B4})$$

Eq. (B3) is rewritten as

$$\Lambda(p) = U - \frac{1}{h \chi(0)} \int d\omega \left[ \frac{1}{p_0 + h/2 - \omega} - \frac{1}{p_0 - h/2 - \omega} \right] \Omega_0(\omega, \mathbf{p}). \quad (\text{B5})$$

Here, we also used the relation

$$\Omega_0(-\omega, \mathbf{p}) = \Omega_0(\omega, \mathbf{p}). \quad (\text{B6})$$

In the case of no external field, Eq. (B5) is reduced, by taking the limit of  $h \rightarrow 0$ , to

$$\Lambda(p) = U - \frac{1}{\chi(0)} \frac{\partial}{\partial p_0} \int d\omega \frac{1}{p_0 - \omega} \Omega_0(\omega, \mathbf{p}). \quad (\text{B7})$$

Let us now renormalize the function  $\Lambda(p)$ . When the renormalization condition (3.25) is imposed on the vertex function,  $\Lambda(p)$  have to satisfy the relation from Eqs. (3.25), (B1), and (B7):

$$U_r = \Lambda(0, \mathbf{p}_F) = U - \left[ \frac{1}{\chi(0)} \frac{\partial}{\partial p_0} \int d\omega \frac{1}{p_0 - \omega} \Omega_0(\omega, \mathbf{p}_F) \right]_{p_0=0, T=T_c}, \quad (\text{B8})$$

Thus, eliminating the bare coupling constant  $U$  in (B7) by the use of Eq. (B8), we obtain the following renormalized function  $\Lambda_r(p)$ :

$$\Lambda_r(p) = U_r + \left[ \frac{1}{\chi(0)} \frac{\partial}{\partial p_0} \times \int d\omega \frac{1}{p_0 - \omega} \Omega_0(\omega, \mathbf{p}_F) \right]_{p_0=0, T=T_c} \quad (\text{B9})$$

The function  $\Theta^{ab}(p)$  in Eq. (3.7) can be obtained as follows. Using Eq. (3.26), we have

$$\text{Re}\Gamma_{\xi\eta\zeta}^{\xi\eta\zeta}(p; -p)\delta^{\xi\eta}\delta^{\xi\zeta} = \left[ \Theta_1(p)\Theta_1(-p) + \pi^2\theta(p)\theta(-p) \right. \\ \left. \times \left[ \frac{e^{p_0/T} - 1}{e^{p_0/T} + 1} \right]^2 \right] \delta^{\xi\eta}\delta^{\xi\zeta}\tau_2. \quad (\text{B10})$$

Considering Eqs. (B1) and (B10), we request the relation,

$$\Theta_1(p)\Theta_1(-p) + \pi^2\theta(p)\theta(-p) \left[ \frac{e^{pp_0/T} - 1}{e^{p_0/T} + 1} \right]^2 = \Lambda_r(p). \quad (\text{B11})$$

In the low-energy region where we are concerned with the second term is very small, because  $e^{p_0/T} - 1 \approx 0$  for  $p_0 \approx 0$ . Thus, neglecting the second term on the left-hand side of Eq. (B11), we have

$$\Theta_1(p) = \sqrt{\Lambda_r(p)}. \quad (\text{B12})$$

Here we assumed  $\Theta_1(p) = \Theta_1(-p)$  for simplicity. The spectral function  $\theta(p)$  can be obtained from the dispersion relation,

$$\theta(p) = - \int d\omega \frac{1}{p_0 - \omega} \sqrt{\Lambda_r(p)}. \quad (\text{B13})$$

- <sup>1</sup>See, for example, *Proceedings of the International Conference on Low Temperature Physics* [Jpn. J. Appl. Phys. **26**, Suppl. 26-3, 993 (1987)]; *Proceedings of the Eighteenth Yamada Conference on Superconductivity in Highly Correlated Fermion Systems, Sendai, Japan, 1987*, edited by M. Tachiki, Y. Muto, and S. Maekawa [Physica B **148** (1987)]; *Novel Superconductivity*, edited by S. A. Wolf and V. Z. Kresin (Plenum, New York, 1987).
- <sup>2</sup>C. E. Gough, M. S. Colclough, E. M. Forgan, R. G. Jordan, P. M. Keene, C. M. Muirhead, A. I. M. Rae, N. Thomas, J. S. Abell, and S. Sutton, *Nature* (London) **326**, 855 (1987).
- <sup>3</sup>J. S. Tsai, Y. Kubo, and J. Tabuchi, *Phys. Rev. Lett.* **58**, 1979 (1987).
- <sup>4</sup>T. Yamashita, A. Kawasaki, T. Nishihara, Y. Hirotsu, and M. Takata, *Jpn. J. Appl. Phys.* **26**, L635 (1987).
- <sup>5</sup>Y. Iye, T. Tamegai, H. Takeya, and H. Takei, *Physica B* **148**, 224 (1987).
- <sup>6</sup>Y. Hidaka, M. Oda, M. Suzuki, A. Katsui, T. Murakami, N. Kobayashi, and M. Muto, *Physica B* **148**, 329 (1987).
- <sup>7</sup>Y. Koike, T. Nakanomyo, and T. Fukase, *Jpn. J. Appl. Phys.* **27**, L841 (1988).
- <sup>8</sup>A. Junod, A. Bezing, and J. Muller, *Physica C* **152**, 50 (1988).
- <sup>9</sup>S. E. Inderhees, M. B. Salamon, Nigel Goldenfeld, J. P. Rice, B. G. Pazol, D. M. Ginsberg, J. Z. Liu, and G. W. Crabtree, *Phys. Rev. Lett.* **60**, 1178 (1988).
- <sup>10</sup>See, for example, P. J. M. van Bentum, L. E. C. van de Leemput, L. W. M. Schenrs, P. A. A. Teunissen, and H. van Kempen, *Phys. Rev. B* **36**, 843 (1987).
- <sup>11</sup>D. R. Harshmann, G. Aeppli, E. J. Ansaldo, B. Batrog, J. H. Brewer, J. F. Carolan, R. J. Cava, M. Celio, A. C. D. Chaklader, W. N. Hardy, S. R. Kreitzman, G. M. Luke, D. R. Noakes, and M. Senba, *Phys. Rev. B* **36**, 2386 (1987).
- <sup>12</sup>Y. J. Uemura, W. J. Kossler, X. H. Yu, J. R. Kempton, H. E. Schone, D. Opie, C. E. Stronach, D. C. Johnston, M. S. Alvarez, and D. P. Goshorn, *Phys. Rev. Lett.* **59**, 1045 (1987).
- <sup>13</sup>W. J. Kossler, J. R. Kempton, X. H. Yu, H. E. Schone, Y. J.

- Uemura, A. R. Moodenbaugh, M. Suenaga, and C. E. Stronach, *Phys. Rev. B* **35**, 7133 (1987).
- <sup>14</sup>W. W. Warren, Jr., R. E. Walstedt, G. F. Brennert, G. P. Espinosa, and J. P. Remeica, *Phys. Rev. Lett.* **59**, 1860 (1987).
- <sup>15</sup>M. Mali, D. Brinkmann, L. Pauli, J. Roos, H. Zimmermann, and J. Hullinger, *Phys. Lett. A* **124**, 112 (1987).
- <sup>16</sup>Y. Kitaoka, S. Hiramatsu, T. Kondo, and K. Asayama, *J. Phys. Soc. Jpn.* **57**, 31 (1988).
- <sup>17</sup>T. Imai, T. Shimizu, T. Tsuda, H. Yasuoka, T. Takabatake, Y. Nakazawa, and M. Ishikawa, *J. Phys. Soc. Jpn.* **57**, 1771 (1988); T. Imai, T. Shimizu, H. Yasuoka, Y. Ueda, and K. Kosuge, *ibid.* **57**, 2280 (1988).
- <sup>18</sup>J. Suzumura, Y. Hasegawa, and H. Fukuyama (private communication).
- <sup>19</sup>Y. Takahashi and H. Umezawa, *Collect. Phenom.* **2**, 55 (1975).
- <sup>20</sup>H. Umezawa, H. Matsumoto, and M. Tachiki, *Thermo Field Dynamics and Condensed States* (North-Holland, Amsterdam, 1982).
- <sup>21</sup>T. Koyama and M. Tachiki, *Phys. Rev. B* **36**, 437 (1987).
- <sup>22</sup>T. Koyama and M. Tachiki, *Jpn. J. Appl. Phys.* **26**, Suppl. 26-3, 475 (1987).
- <sup>23</sup>H. Matsumoto, *Fortschr. Phys.* **25**, 1 (1977).
- <sup>24</sup>J. R. Schrieffer, *Theory of Superconductivity* (Benjamin, New York, 1964).
- <sup>25</sup>The vertex function  $\Gamma_{\xi\eta\zeta}^{\xi\eta\zeta}(-p-q;p)$  introduced in Eq. (2.16) is related to  $\Gamma_{\xi\eta\zeta}^{\xi\eta\zeta}(p;-p-q)$  by the relation,  $\Gamma_{\xi\eta\zeta}^{\xi\eta\zeta}(-p-q;p) = \Gamma_{\xi\eta\zeta}^{\xi\eta\zeta}(p;-p-q)$ .
- <sup>26</sup>J. Whitehead, H. Matsumoto, and H. Umezawa, *Phys. Rev. B* **25**, 4737 (1982).
- <sup>27</sup>See Chap. 6 in Ref. 20.
- <sup>28</sup>R. E. Walstedt, W. W. Warren, Jr., R. F. Bell, G. F. Brennert, G. P. Espinosa, R. J. Cava, L. F. Schneemeyer, and J. V. Waszczak (unpublished).